Tetrahedron 66 (2010) 5212–5217

Contents lists available at ScienceDirect

Tetrahedron

journal homepage: www.elsevier.com/locate/tet

Ground state potential energy surface between cyclobutadiene and tetrahedrane looked down from S_1/S_0 conical intersections

Masato Sumita [†], Kazuya Saito [*]

Department of Chemistry, Graduate School of Pure and Applied Sciences, University of Tsukuba, Tsukuba, Ibaraki 305-8571, Japan

ARTICLE INFO

Article history:
Received 25 March 2010
Received in revised form 20 April 2010
Accepted 20 April 2010
Available online 24 April 2010

ABSTRACT

We have explored the singlet ground state potential energy surface (S_0 PES) between cyclobutadiene (CBD) and tetrahedrane (THD) looked down from S_1/S_0 conical intersections through multi-configuration self-consistent field theory. On the basis of the obtained S_0 PES, we propose the revised process of the THD to CBD symmetry-forbidden reaction. According to the present result, the THD to CBD rearrangement occurs via plural steps similarly to previous suggestions, but via a tetra-radical species (instead of an *endo*-species), which is considered for the first time in this paper. Since the *endo*-species is significantly destabilized when hydrogen atoms are replaced by bulky substituents (such as *tert*-butyl group), the present one, where *endo*-species are not involved, would be realized in actual systems having bulky substituents.

1. Introduction

Cyclobutadiene (CBD) is a very interesting simple molecule. Many theoretical and experimental chemists often regard it as an anti-aromatic paradigm[1–3] because CBD is a typical antiaromatic molecule in view of Hückel rule. In spite of its simplicity, the structure of CBD has not been established experimentally because of its instability. However, many theoretical and experimental results suggest that its structure should be rectangular D_{2h} in the singlet ground state (S_0).[4–14]

Although the property of the unsubstituted CBD is still uncertain, relatively stable derivatives of CBD show very interesting photochemical properties. That is, the derivatives having bulky substituents isomerize to corresponding derivatives of tetrahedrane (THD).[15–20] For example, tetra-*tert*-butyl CBD isomerizes to tetra-*tert*-butyl THD with light of wavelength >300 nm (<4.12 eV)[15] as shown in Scheme 1. The CBD to THD rearrangement is a symmetry-forbidden reaction since the occupied and unoccupied orbitals should be crossed during this arrangement as seen in the orbital correlation diagram in Figure 1. Hence, this rearrangement is

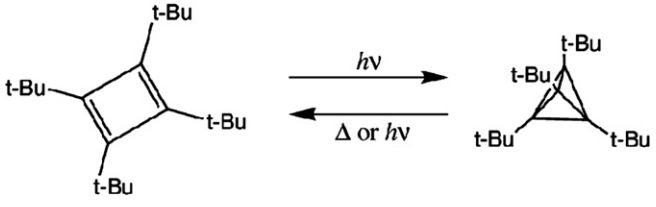

Scheme 1.

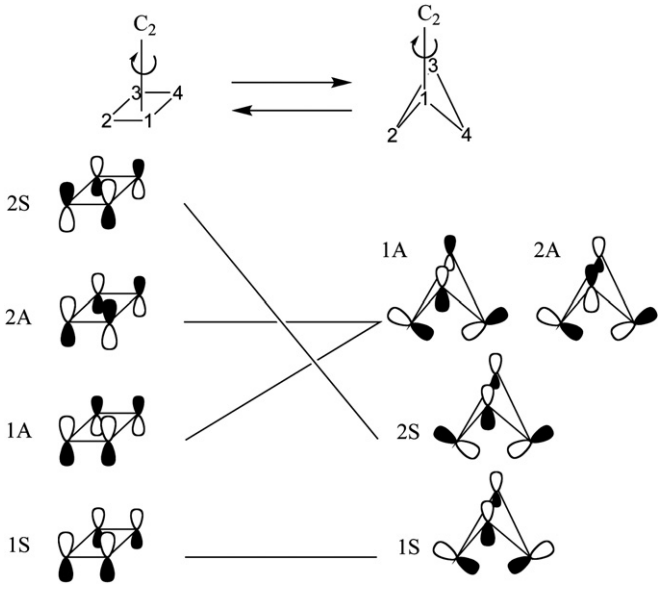

Figure 1. Orbital correlation diagram between CBD and THD. The sign of 'A' and 'S', which denote 'Anti-symmetry' and 'Symmetry,' respectively, are assigned to orbitals assuming C_2 symmetry. In CBD (left side), 1S and 1A orbitals are doubly occupied and 2A and 2S are empty (virtual). In THD (right side), 1S and 2S orbitals are doubly occupied and 1A and 2A are empty. When THD↔CBD rearrangement occurs, the occupied orbital should intersect the virtual orbital.

* Corresponding author. Tel.: +81 29 853 4239; fax: +81 29 853 6503; e-mail address: kazuya@chem.tsukuba.ac.jp (K. Saito).
† Present address: National Institute for Materials Science (NIMS), 1-1 Namiki, Tsukuba, Ibaraki 305-0044, Japan.

0040-4020/$ – see front matter © 2010 Elsevier Ltd. All rights reserved.
doi:10.1016/j.tet.2010.04.083

achieved only by light irradiation. However, the reverse reaction, tetra-*tert*-butyl THD to tetra-*tert*-butyl CBD, occurs thermally (Scheme 1) though it is also symmetry-forbidden.[15–20]

Some chemists[16,21,22] attempted to elucidate this reaction processes by calculating the THD to CBD rearrangement as a model of that of the tetra-*tert*-butyl THD to CBD, etc. We consider that this selection of a model system is adequate, on the basis of our preliminary calculation,[23] which showed that the electronic structure of tetra-*tert*-butyl CBD is very similar to that of CBD. Furthermore, by exploring the reaction process from THD to CBD, we possibly examine whether the unsubstituted THD, which has never been isolated, is synthesizable or not.

According to the previous calculations,[16,21,22] it is widely assumed that the THD to CBD rearrangement process proceed via the following plural steps (Scheme 2): first, by breaking of one bond of THD (**2**), *exo*-bicyclodiracial is produced. Second, the *exo*-bicyclodiradical converts to an *endo*-species. Finally, the *endo*-species isomerizes to CBD (**1**).

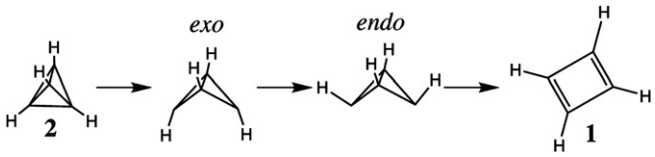

Scheme 2.

The estimated activation energies differs significantly depending on employed computational methods, ab initio or semi-empirical. The energy of the reaction-rate controlling transition state (TS) calculated by ab initio calculations (HF, MP2)[16,21] is about 230 kJ mol^{-1} with respect to CBD, which is approximately twice that calculated by a semi-empirical calculation (MINDO/3).[21] Kollmar et al.[21] claimed that the activation energy should be larger for THDs with bulky substituents than this estimate because the intermediate species are destabilized due to the steric repulsion between the bulky groups. Considering the destabilization due to such steric repulsion, the activation energy for tetra-*tert*-butyl THD to CBD may become too large to occur. However, in this paper, we will propose the reaction process that is less affected by the steric repulsion between bulky groups.

The previous calculations[16,21,22] have certainly some weak points. First, the calculations of the PES were done by single-determinant based methods, i.e., HF, MP2, and MINDO/3. Since the crossing (degeneracy) between the occupied and unoccupied orbital is expected in the rearrangement, as shown in Figure 1, multi-configuration based calculation [e.g., the complete active space self-consistent field (CASSCF) theory] is more suitable for the theoretical analysis of this system.[24] Second, the previous calculations imposed C_2 symmetry on the system with a fixed symmetry axis. According to our prediction, a distorted structure from such C_2 symmetry (shown in Fig. 1) would be involved in the reaction process. Then, the HOMO of CBD (1A) should intersect (degenerate with) the next LUMO (2S) as shown in Figure 1. Considering the linear combination between the HOMO and next LUMO, therefore, THD would isomerize to CBD via an ionic TS as in Figure 2. This TS is hardly searched while imposing the C_2 symmetry because the C_2 symmetry axis of this TS is different from the assumed one of those of CBD (normal to the CBD plane). As will be shown, an ionic TS has been located from the tetra-radical species, which exist in the vicinity of a conical intersection (CI) between the ground state (S_0) and first excited state (S_1) of CBD.[23]

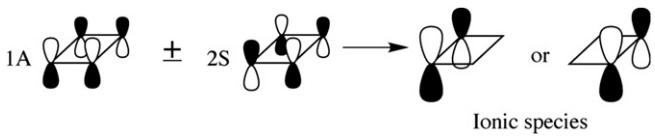

Figure 2. Qualitative linear combination between 1A and 2S orbitals of CBD. From this, it is considered that the ionic species would be involved in the THD to CBD rearrangement.

In recent years, theoretical chemists have revealed the importance of CIs, real crossing between potential energy surfaces (PESs), as already predicted by Teller several decades ago.[25] The existence of CIs makes it possible to explain sub pico-second-order ultra fast photo-induced processes because the barrierless non-adiabatic transition without emission of light is possible at CIs.[26–28] The *cis–trans* photoisomerization of the retinal protonated Schiff base is a well-known example.[29–31] However, some recent theoretical calculations demonstrated that the CIs also affect directly thermal reactions. Namely, some thermal reaction is hindered because an upward transition from the ground to first excited state is possible at the CIs.[32–35] This is called as a non-adiabatic trapping effect.

In this paper, we report the analysis of thermal reaction process expected for the THD to CBD rearrangement on the basis of a ground state (S_0) PES looked down from CIs, though we do not report the direct involvement of the CIs in the process. Considering that CIs would be the highest points on the ground PES, placing CIs on the PES at the first stage makes easier the analysis of the thermal reaction process. This paper will demonstrate the importance of locating CI even in analyses of thermal reactions and propose the revised mechanism of the THD to CBD rearrangement on the S_0 PES.

2. Computational details

Geometry optimization, minimum-energy-path (MEP) calculation, and intrinsic reaction coordinate (IRC) calculation were performed using the complete active space self-consistent filed (CASSCF) method implemented in Gaussian03.[36] The feature of CASSCF is the flexibility in selecting an appropriate active space. One should select orbitals as an active space suitably.

The optimized geometry of CBD by CASSCF,[37] where the π system (four electrons in four orbitals) was employed as the active space, did not agree with the result of the calculation that includes dynamical electronic correlation (CCSD).[38] In order to reduce this disagreement, eight π electrons in eight π orbitals that correspond to the π system of two acethylenes, i.e., the four π electrons in four π orbitals and four σ electrons in four σ orbitals were used as the active space [CAS(8,8)]. The result of CASSCF appeared to be improved by adding the σ orbital to the active space.[23] That is, the optimized structure of CBD by CAS(8,8) is comparable to that by CCSD.[38]

To describe the 6 equivalent σ bonds of THD accurately, 12 electrons in 12 orbitals are preferable as an active space. However, such an active space is demanding even for modern computers. We expected that the result in this paper [CAS(8,8)] would not be different significantly from that of CAS(12,12) because we do keep off the breakage of the σ bonds that constructs the original σ bonds of CBD.

According to Ref. 38, there are no marked difference in resultant geometries between CCSD calculations with cc-pVDZ and cc-pVTZ except for the C–H bonds. Hence, we adopted cc-pVDZ as the basis set throughout this work.

CASSCF calculation takes into account the non-dynamic electronic correlation, but not dynamic electronic correlation properly. To make the result of calculation more reliable, it is necessary to include the effect of dynamic electronic correlation. The results of the CASSCF calculation showed that electronic structures have multi-configuration property at some stationary points on the S_0 PES we have located. This means that multi-reference calculation is more suitable. Hence, to improve the computed energetics by incorporating the effect of the dynamic electronic correlation, we have carried out single point calculations using multi-reference Møller–Plesset second-order perturbation (MRMP2)[39] implemented in GAMESS[40] on the CASSCF-optimized geometries. A

reference CASSCF/cc-pVDZ wave function with the same active space described above was used for all MRMP2 calculations. The weights of states in MRMP2 were equally assigned for three states (S_0, S_1, and S_2) for consistent comparison with the energies of the CIs.

3. Result and discussion

Hereafter, the atomic numbering for carbon is used as shown in Figures 1, 5, and 6. That for the hydrogen atoms uses the number of the carbon it attached to. The geometric parameters, energies, and Mulliken charges of carbon atoms at the stationary points we have located are tabulated in Tables 1–3, respectively. Each species is discriminated by assigning the bold Arabic numerals. The bold Arabic numerals with prime indicate the TSs. The reaction process we report in this paper is schematically summarized in Figure 5.

3.1. S_0 MEPs from the S_1/S_0 CIs of CBD

First of all, we should report the S_0 MEP calculations from the S_1/S_0 CIs of CBD. We had already located the two CIs; ionic CI (CI_{ionic}) and tetra-radical CI (CI_{tetra}).[23] CI_{ionic} is found as the terminal point of the S_1 MEP from the Frank–Condon state by CASSCF. The π electrons of CI_{ionic} are biased to the two diagonally opposite carbon atoms. The structure at CI_{ionic} is rhomboid as shown in Figure 3. In

Table 1
Geometric parameters of cyclobutadiene (CBD), S_1/S_0 conical intersections, and other stationary points optimized by CAS(8,8)/cc-pVDZ implemented in Gaussian03

	CBD (**1**)	CI_{ionic}	CI_{tetra}	**5′**	**4**	**4′**	**3**	**3′**	THD(**2**)	**6′**	**6**	**7′**
Bond length (Å)												
C1–C2	1.35	1.47	1.53	1.58	1.48	1.48	1.49	1.48	1.51	1.45	1.43	1.50
C2–C3	1.59	1.44	1.46	1.48	1.44	1.44	1.45	1.44	1.47	1.44	1.47	1.45
C3–C4	1.35	1.47	1.53	1.41	1.48	1.48	1.49	1.48	1.51	1.45	1.43	1.50
C4–C1	1.59	1.44	1.49	1.48	1.44	1.44	1.45	1.44	1.47	1.44	1.47	1.45
C1–H1	1.08	1.09	1.09	1.09	1.08	1.08	1.07	1.07	1.07	1.08	1.09	1.08
C2–H2	1.08	1.08	1.08	1.09	1.08	1.08	1.09	1.07	1.07	1.08	1.08	1.08
C3–H3	1.08	1.09	1.08	1.08	1.08	1.08	1.07	1.07	1.07	1.08	1.09	1.08
C4–H4	1.08	1.08	1.09	1.08	1.08	1.08	1.09	1.07	1.07	1.08	1.08	1.08
C1–C3	2.09	1.86	2.07	2.00	1.83	1.79	1.56	1.57	1.51	1.68	1.71	1.73
C2–C4	2.09	2.18	2.07	2.00	1.83	1.86	1.91	1.67	1.47	2.25	2.23	2.29
Sum of the bond angles around carbon atoms (°)												
Σ_{C1}[a]	360.0	356.6	332.6	314.1	336.6	333.8	360.0	337.0	347.0	354.4	354.7	347.3
Σ_{C2}[a]	360.0	338.3	344.2	314.1	336.6	340.8	327.3	354.8	350.6	319.1	322.2	340.4
Σ_{C3}[a]	360.0	356.6	344.2	359.4	336.6	333.8	360.0	359.4	350.6	354.4	354.8	347.3
Σ_{C4}[a]	360.0	338.3	332.6	359.4	336.6	340.8	327.3	354.8	350.6	319.1	322.2	340.5
Dihedral angle (°)												
C1–C2–C3–C4	0.0	18.9	24.8	36.6	49.4	49.7	56.4	62.0	67.5	29.0	27.9	26.6
H1–C1–C2–H2	0.0	7.8	−118.0	−159.2	−147.6	−146.4	−113.0	−81.8	−5.9	5.7	6.1	−109.5
H2–C2–C3–H3	0.0	−8.5	106.6	109.1	146.8	145.5	111.0	78.4	0.0	−7.7	−8.6	110.0
H3–C3–C4–H4	0.0	7.8	−118.0	−53.9	−147.6	−146.4	−112.9	−81.8	−5.9	5.7	6.0	−109.4
H4–C4–C1–H1	0.0	−8.5	129.5	−109.1	146.8	145.5	111.0	78.4	0.0	−7.7	−8.6	110.0

[a] Sum of the bond angle around a carbon atom.

Table 2
CAS(8,8)/cc-pVDZ and MRMP2//CAS(8,8)/cc-pVDZ energies for cyclobutadiene (CBD), S_1/S_0 conical intersections, and other stationary points

Species	State	E_{CAS}[a]	E_{CAS}[b]	E_{CAS}[c]	E_{MRMP2}[d]	E_{rel}[e]
CBD (**1**)	S_0	−153.77413	—	−153.76684	−154.20179	0(0)
	S_1	—	—	−153.61701	—	(393.39)
CI_{ionic}[f]	S_0	—	−153.70294	−153.70493	−154.15040	134.91(162.56)
	S_1	—	−153.70294	−153.69349	−154.14195	157.08(192.61)
CI_{tetra}[f]	S_0	—	−153.63570	−153.63127	−154.09954	297.33(355.96)
	S_1	—	−153.63570	−153.62925	−154.08469	307.45(361.24)
5′	S_0	−153.65448(1186i)	—	−153.64346	−154.10244	260.83(323.95)
	S_1	—	—	−153.58437	—	(479.09)
4	S_0	−153.69496	—	−153.68257	−154.14415	151.33(221.27)
	S_1	—	—	−153.45547	—	(817.53)
4′	S_0	−153.69495(154i)	—	−153.68242	−154.14420	151.19(221.67)
	S_1	—	—	−153.46438	—	(794.14)
3	S_0	−153.69836	—	−153.67887	−154.14840	140.17(230.99)
	S_1	—	—	−153.46297	—	(797.83)
3′	S_0	−153.69419(540i)	—	−153.67183	−154.14466	149.99(249.46)
	S_1	—	—	−153.37018	—	(1041.44)
THD(**2**)	S_0	−153.70040	—	−153.65625	−154.15076	133.99(290.36)
	S_1	—	—	−153.37569	—	(1026.99)
6	S_0	−153.72182	—	−153.70575	−154.16742	90.24(160.4)
	S_1	—	—	−153.60373	—	(428.2)
6′	S_0	−153.72170(395i)	—	−153.70454	−154.16485	96.98(163.59)
	S_1	—	—	−153.61807	—	(390.61)
7′	S_0	−153.64975(837i)	—	−153.63831	−154.10326	258.69(337.5)
	S_1	—	—	−153.56461	—	(531.0)

[a] Single-state CASSCF energy in atomic units (computed by Gaissian03). Values of imaginary frequency (cm^{-1}) are shown in parentheses.
[b] Two-state-averaged CASSCF energy for S_0 and S_1 in atomic units (computed by Gaissian03).
[c] Three-state-averaged CASSCF energy for S_0, S_1, and S_2 in atomic units (computed by GAMESS).
[d] MRMP2 energy for S_0, S_1, and S_2 in atomic units (computed by GAMESS).
[e] MRMP2 relative energy with respect to the S_0 equilibrium structure of CBD in kJ mol^{-1}. The values in parentheses are those of the three-state-averaged CASSCF energy.
[f] Geometries are obtained by two-state-averaged CASSCF (Gaissian03).

Table 3
Mulliken charges of carbon atoms calculated by CASSCF at each species in atomic units

	CBD(**1**)	**5′**	**4**	**4′**	**3**	**3′**	THD(**2**)	**6′**	**6**	**7′**
C1	−0.0204	−0.0637	−0.0689	−0.0596	−0.0285	−0.0404	−0.0261	0.0194	0.0123	−0.0425
C2	−0.0204	−0.0637	−0.0689	−0.0766	−0.0679	−0.0406	−0.0261	−0.1134	−0.1096	−0.0815
C3	−0.0204	−0.0340	−0.0689	−0.0596	−0.0285	−0.0404	−0.0261	0.0194	0.0123	−0.0425
C4	−0.0204	−0.0340	−0.0689	−0.0766	−0.0678	−0.0406	−0.0261	−0.1134	−0.1096	−0.0817

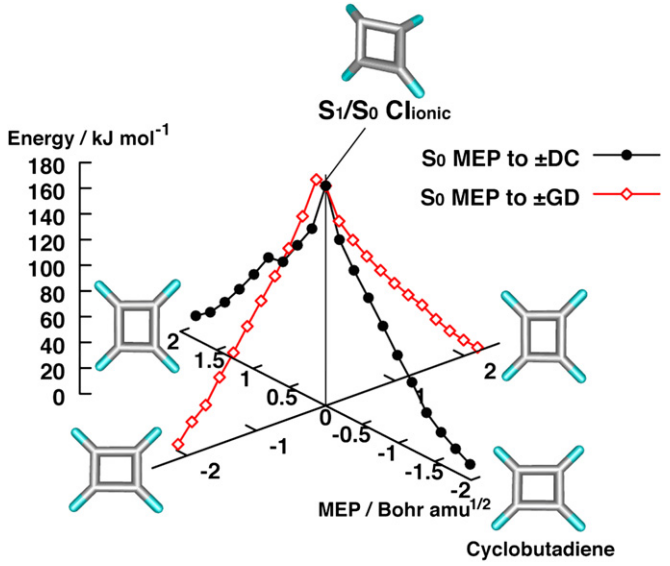

Figure 3. S_0 minimum-energy-path (MEP) from the CI_{ionic} with the initial direction to its ±GD and ±DC by CASSCF. We depicted this picture by making the ±GD axis perpendicular to the ±DC axis.

CI_{tetra}, four π electrons seem to be assigned equally to the four carbon atoms. This electronic structure results in pyramidalized carbon atoms. Consequently, the hydrogen atoms are alternately attached to the four-membered ring from the up and down sides of the ring as shown in Figure 4.

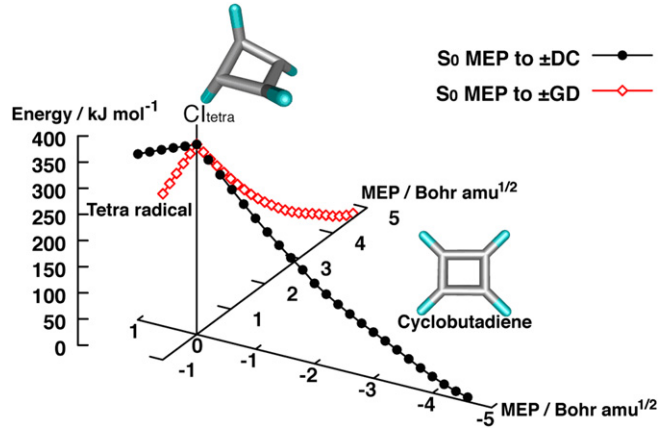

Figure 4. S_0 minimum-energy-path (MEP) from the CI_{tetra} with the initial direction to its ±GD and ±DC by CASSCF. We depicted this picture by making the ±GD axis perpendicular to the ±DC axis.

We carried out the S_0 MEP calculation in the mass-weighted coordinate from these S_1/S_0 CIs of CBD. MEP calculations make it possible to explore the reaction path within the first-order displacement at the starting point. At CIs, one can define the two internal coordinates of the molecule that lift the degeneracy.[26–28] One is the gradient difference vector (GD; $\boldsymbol{g}$),

$$\boldsymbol{g} = \frac{\partial(E_1 - E_0)}{\partial \boldsymbol{R}}, \tag{1}$$

where E_1 and E_0 are the upper and lower energies, respectively, $\boldsymbol{R}$ the coordinate of nuclei. The other is the derivative coupling vector (DC;$\boldsymbol{h}$),

$$\boldsymbol{h} = \left\langle \Psi_0 \left| \frac{\partial}{\partial \boldsymbol{R}} \Psi_1 \right. \right\rangle, \tag{2}$$

where, H is the electronic Hamiltonian, Ψ_1 and Ψ_0 are wave function of the upper and lower sates, respectively. Hence, we have carried out S_0 MEP calculations by putting an initial displacement along one of ±GD and ±DC at each CI.

The results of the S_0 MEP calculations from CI_{ionic} are shown in Figure 3. The S_0 MEP with an initial displacement to −GD shows the barrier in an early stage of this path. This fact may indicate that CI_{ionic} has property of the so-called sloped CI.[41] All the S_0 MEPs show that CBD via CI_{ionic} undergoes the automerization as we already predicted in a previous paper.[23] The single- and double-bonds of CBD reached in S_0 MEP with an initial displacement to −GD or −DC are alternated with those reached in S_0 MEP with an opposite initial displacement (+GD or +DC). The TS, which corresponds to **6′** as will be shown later, can be located in the direction to +GD. This TS has the *endo*-bicyclo structure and is similar to that of the TS that leads CBD to *endo*-species and was reported by Kollmar et al.[21,22] Vibrational analysis shows that the imaginary frequency of **6′** is 395i cm^{-1} and represents H1 and H3 wagging motion.

The results of the S_0 MEP calculations from CI_{tetra} are shown in Figure 4. The product obtained from S_0 MEP with an initial displacement along +GD or −DC is CBD (no automerization). On the other hand, S_0 MEP calculation with an opposite initial displacement (−GD or +DC) failed in the vicinity of CI_{tetra} (<1.0 Bohr $amu^{1/2}$) although the molecular structure tends to distort in a more tetra-radical like manner. We therefore carried out geometry optimizations from the final points of the S_0 MEP calculations in the directions to −GD and +DC. We obtained an energy minimum that has a bicyclodiradical structure (**3**), whose electronic structure corresponds to the bicyclodiracial located previously by Kollmar et al.[21,22] This bicyclodiracial lies 140.2 kJ mol^{-1} above CBD and only 6.2 kJ mol^{-1} above THD at the MRMP2//CASSCF level.

We also carried out TS searching calculation from the final point of the S_0 MEPs with initial displacements to +DC and −GD. In the direction to −GD, we have located the TS (**7′**) that leads *endo*-bicyclo-species to *exo*-bicyclodiradical species. TS **7′** has already been located by Kollmar et al.[16,21,22] Therefore, CI_{tetra} is certainly involved in the criss-cross reaction of CBD. On the other hand, we have located a tetra-radical like TS (**4′**) in the direction to +DC, which has never been located previously. The IRC calculation indicated that **4′** leads a bicyclodiradical intermediate (**3**) to a tetra-radical intermediate (**4**), which is reached only after the intersection of the HOMO (1A) and next LUMO (2S) in CBD. Hence, these tetra-radical species (**4** and **4′**) are expected to be intermediate or TS on the course to THD. The details of **4** and **4′** are described in the next section.

3.2. Rearrangement from THD to CBD via tetra-radical species

The isomerization process from THD (**2**) to CBD (**1**) we propose in this paper is summarized in Figure 5, which helps reading this section.

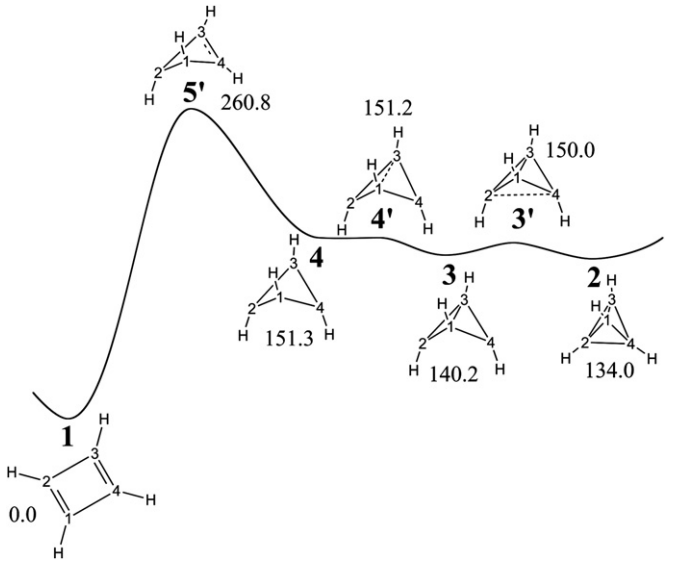

Figure 5. Schematic representation of the S_0 potential energy surface in the THD/CBD system with the relative energies to CBD (in kJ mol^{-1}) along the path newly proposed. Bold Arabic numerals are to discriminate species. Bold Arabic numerals with prime indicate transition state species.

Tetra-radical species (**4** and **4′**), which is to be involved in the THD to CBD rearrangement, were found from CI_{tetra}. We have found that the TS (**5′**) leads the tetra-radical intermediate (**4**) to CBD. This TS is the ionic TS as we expected.

TS **5′**, which lies 260.8 kJ mol^{-1} above CBD and 109.5 kJ mol^{-1} above **4** at the MRMP2//CASSCF level, can be easily located by QST2 strategy.[36] The imaginary frequency of **5′** was calculated as 1186i cm^{-1} and represents the hydrogen rocking motion at the CASSCF level. Its electronic structure agreed with our qualitative predication. Namely, electrons are biased to C1 and C2. The charges of C1 and C2 are −0.064 a.u. Consequently, C1 and C2 have sp^3 character ($\Sigma_{C1,C2}$=314° in Table 1). The relation between CBD, **5′**, and **4** was confirmed by the IRC calculation at the CAS(8,8) level.

TS **4′** was also located in the direction to the C1–C3 length shortening of **4** at the CAS(8,8) level. The imaginary frequency of **4′** is 154i cm^{-1} and represents the stretching of the C1–C3 bond. However, the estimated energy of **4′** at the MRMP2//CASSCF level is slightly lower than that of **4** (by 0.14 kJ mol^{-1}). Therefore, the S_0 PES between **4** and **4′** is flat. The IRC calculation at the CASSCF level indicated that an *exo*-bicyclodiradical intermediate (**3**) is produced via **4′** from **4**. Intermediate **3** lies only 11 kJ mol^{-1} below **4** and **4′**. The *exo*-bicyclodiradical **3** is linked to THD via the TS involved in the C2–C4 bond breaking/making (**3′**) similarly to the previous calculations.[21,22] TS **3′** has been located in the direction to the C2–C4 bond shortening of **3**.

At the CAS(8,8) level, the imaginary frequency of **3′** is 540i cm^{-1} and represents the C2–C4 bond breaking/making. MRMP2//CASSCF calculation indicates that **3′** lies 9.8 kJ mol^{-1} above the *exo*-bicyclodiradical intermediate (**3**). Furthermore, the IRC calculation indicated that **3′** leads **3** to THD (**2**). The energy of THD is calculated as 134 kJ mol^{-1} with respect to CBD at the MRMP2//CASSCF level. Therefore, the barrier for breaking of the single bond of THD is only 16 kJ mol^{-1}. This value is extremely smaller than those calculated by MINDO/3 and HF.[21,22,42]

We summarized the new reaction process in Figure 5. First, one σ bond (C2–C4) of THD (**2**) is broken and THD changes into the bicyclodiradical intermediate (**3**). The σ bond (C1–C3) of **3** is broken again and **3** changes into the tetra-radical species (**4** or **4′**). At the CASSCF level, the tetra-radical intermediate structure (**4**) is expected. However, the MRMP2//CASSCF calculations indicated that **4** is possibly non-stationary. In any way, the tetra-radical species changes into CBD (**1**) via the ionic TS (**5′**).

3.3. Comparison with the previous reaction processes

In order to compare the reaction process proposed in this paper with the reaction process previously proposed, we have located by CASSCF the stationary points (**6**, **6′**, and **7′**) appeared in the old process[16,21,22] and these energies have recalculated by the MRMP2 (**7′** was located starting from the CI_{tetra}). The results are compared with the previous calculations in Table 4. We confirmed the reactant/product relations by IRC calculations at the CASSCF level. The schematic energy diagram depicted on the basis of MRMP2//CASSCF calculations is shown in Figure 6.

Table 4
Comparison with previous calculation data in kJ mol^{-1}

	MP2[a]	MINDO/3[b]	MRMP2[c]
CBD (**1**)	0	0	0
6′	89.5	61.1	97.0
6	71.5	59.0	90.2
7′	236	179	258.7
3	100	173	140.2
3′	100	178	150.0
THD (**2**)	95.8	133	134.0

[a] Ref. 16.
[b] Ref. 21.
[c] This paper.

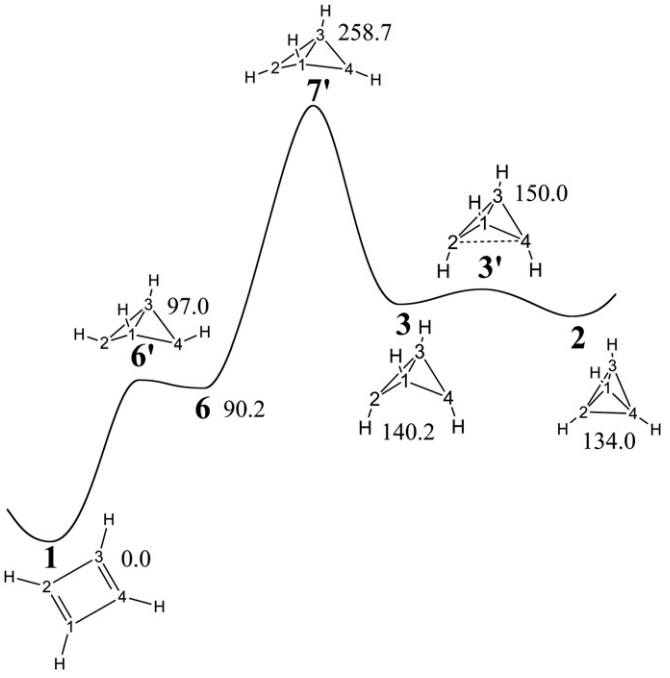

Figure 6. Schematic representation of the S_0 potential energy surface in the THD/CBD system with the relative energies to CBD (in kJ mol^{-1}) along the path previously suggested. Bold Arabic numerals are to discriminate species. Bold Arabic numerals with prime indicate transition state species.

The relative energies of all stationary points obtained by MRMP2//CASSCF are higher than those by the MINDO/3 or MP2 calculations. However, the energy barrier (**7′**) from the side of the *exo*-bicyclo intermediate (**3**) became lower than that by MP2, although the energy of **7′** at the MINDO/3 level is extremely smaller than MRMP2//CASSCF or MP2. The total exothermic energy calculated by MRMP2//CASSCF is 134 kJ mol^{-1}, which is comparable to that by MINDO/3 (133 kJ mol^{-1})[22] and recent B3LYP (110 kJ mol^{-1}).[43] The MP2 calculation seems to underestimate the total exothermic energy.[16,44]

The distance between C1 and C3 of *endo*-bicyclo species (**6**, **6′**, and **7′**) is short (<1.8 Å). This does not mean the bonding between C1 and C3, because electrons are biased to C2 and C4: the charges of C2/C4 at **6** and **6′** are −0.1096 and −0.1134 a.u., respectively. Thus **6** and **6′** appears to be *endo*-bicyclo 'ionic' species. The charges of C2 and C4 decrease down to −0.0817 a.u. around **7′**. Hence, the C1−C3 bond may be formed around **7′**.

The relative energy of the largest barrier in both reaction processes (Figs. 5 and 6) is 259−261 kJ mol^{-1} at the MRMP2//CASSCF level. The highest barrier (**5′**) in the present process is the ionic TS slightly higher than that (**7′**) in the previous process. However, from the foot of the barrier in the side of THD (**2**), the barrier (**5′**) is lower than **7′**. That is to say, the foot of the barrier from the side of THD in the present process (Fig. 5) is tetra-radical species (sit in around 151 kJ mol^{-1} relative to CBD). The energy difference between **5′** and **4** or **4′** is 109 kJ mol^{-1}. On the other hand, the foot of the barrier in the side of THD in the previous process (Fig. 6) is *exo*-bicyclodiracial intermediate (**3**). The energy difference between **7′** and **3** is 119 kJ mol^{-1}.

In actual systems, the hydrogen atoms of THD are replaced by more bulky substitutuents (such as *tert*-butyl group) for stabilization. We have to consider the steric repulsion between bulky substituents, accordingly. Clearly, the *endo*-bicyclo species (**6′**, **6**, and **7**) would be destabilized by the steric repulsion more severely than the *exo*-bicyclodiracial and tetra-radial species (**4**, **4′**, **3**, and **3′**), and the ionic TS (**5′**). Consequently, we conclude that the present reaction process is more feasible than the previous one in realistic systems with bulky substituents.

4. Conclusion

We have shown an analysis of thermal reaction looked down from CIs at the CASSCF level. Although persisting on the ground state PES is a way widely used when we attempt to analyze thermal reactions, looking down from the excited state (conical intersection) brings us to a new view point, from which we can easily realize the existence of the new species. Indeed we have found the new intermediate species, i.e., tetra-radical species of CBD that is concealed under S_1/S_0 CI_{tetra}.

On the basis of this PES, we have proposed a new process of the symmetry-forbidden reaction, THD to CBD. Although the height of the barrier is approximately the same as the reaction process previously suggested, by inserting tetra-radical species into the reaction process, which is found from the S_1/S_0 CI, the barrier is slightly lowered than the previous process from the side of THD. Furthermore, any *endo*-species is not involved along the present process. The *endo*-species are expected to be destabilized severely due to the steric repulsion between bulky substituents when hydrogen atoms are replaced by bulky substituents. Our reaction process is, on the other hand, expected to be less affected by such steric repulsion. Hence, the reaction process that we proposed in this paper for the first time would cover wider situation than the reaction process suggested previously by Kollmar et al.[21,22]

The unsubstituted THD has never been isolated. Although the barrier height of the THD to CBD reaction-rate controlling TS is larger than 100 kJ mol^{-1} in both the present and previous reaction process at the MRMP2//CASSCF level, the barrier for the single-bond breaking in THD is only 16 kJ mol^{-1}. Therefore, it is expected that isolation of the unsubstituted THD is possible only at extremely low temperatures even if it is produced via an excited state.

Supplementary data

The Cartesian coordinates of the stationary points discussed in this paper are tabulated. Results of IRC calculations from the transition states with these three-dimensional descriptions of vibration modes having imaginary frequencies are given. Supplementary data associated with this article can be found, in the online version, at doi:10.1016/j.tet.2010.04.083.

References and notes

1. Bally, T. *Angew. Chem., Int. Ed.* **2006**, *45*, 6616.
2. See all articles in issue 5 of *Chem. Rev.* **2001**, *101*, 1115.
3. See all articles in issue 10 of *Chem. Rev.* **2005**, *105*, 3433.
4. Buenker, R. J.; Peyerimhoff, S. D. *J. Chem. Phys.* **1968**, *48*, 354.
5. Borden, W. T.; Davidson, E. R.; Hart, P. *J. Am. Chem. Soc.* **1978**, *100*, 388.
6. Jafri, J. A.; Newton, M. D. *J. Am. Chem. Soc.* **1978**, *100*, 5012.
7. Schaad, L. J.; Hess, B. A.; Ewig, C. S. *J. Am. Chem. Soc.* **1979**, *101*, 2281.
8. Hess, B. A.; Schaad, L. J.; Čársky, P., Jr. *Pure Appl. Chem.* **1983**, *55*, 253.
9. Hess, B. A.; Čársky, P., Jr.; Schaad, L. J. *J. Am. Chem. Soc.* **1983**, *105*, 695.
10. Masamune, S.; Souto-Bachiller, F. A.; Machiguchi, T.; Berie, J. E. *J. Am. Chem. Soc.* **1978**, *100*, 4889.
11. Maier, G. *Angew. Chem., Int. Ed. Engl.* **1988**, *27*, 309.
12. Balková, A.; Bartlett, R. J. *J. Chem. Phys.* **1994**, *101*, 8972.
13. Sancho-Gracía, J. C.; Pérez-Jiménez, A. J.; Moscardó, F. *Chem. Phys. Lett.* **2000**, *317*, 245.
14. Sancho-Gracía, J. C.; Pittner, J.; Čársky, P.; Hubač, I. *J. Chem. Phys.* **2000**, *112*, 8785.
15. Maier, G.; Neudert, J.; Wolf, O. *Angew. Chem., Int. Ed.* **2001**, *40*, 1674.
16. Maier, G.; Neudert, J.; Wolf, O.; Pappusch, D.; Sekiguchi, A.; Tanaka, M.; Masuo, T. *J. Am. Chem. Soc.* **2002**, *124*, 13819.
17. Maier, G.; Pfriem, S.; Schäfer, U.; Matusch, R. *Angew. Chem., Int. Ed. Engl.* **1978**, *17*, 520.
18. Maier, G.; Born, D. *Angew. Chem., Int. Ed. Engl.* **1989**, *28*, 1050.
19. Maier, G.; Fleischer, F. *Liebigs Ann.* **1995**, 169.
20. Maier, G.; Fleischer, F.; Kalinowski, H. *Liebigs Ann.* **1995**, 173.
21. Kollmar, H.; Carrion, F.; Dewar, M. J. S.; Bingham, R. C. *J. Am. Chem. Soc.* **1981**, *103*, 5292.
22. Kollmar, H. *J. Am. Chem. Soc.* **1980**, *102*, 2617.
23. Sumita, M.; Saito, K. *Chem. Phys.*, in press, doi:10.1016/j.chemphys.2010.03.024.
24. Roos, B. O. In *European Summer School in Quantum Chemistry*; Roos, B. O., Ed.; Lecture Notes in Quantum Chemistry; Springer: Berlin, Heidelberg, 1992; p 177.
25. Teller, E. *J. Phys. Chem.* **1973**, *41*, 109.
26. Bernardi, F.; Olivucci, M.; Robb, M. A. *Chem. Soc. Rev.* **1996**, *25*, 321.
27. Migani, A.; Olivucci, M. In *Conical Intersections: Electronic Structure, Dynamics & Spectroscopy*; Domcke, W., Yarkony, D. R., Köppel, H., Eds.; Advanced Series in Physical Chemistry; World Scientific: Singapore, 2004; Vol. 15, p 271.
28. Yarkony, D. R. In *Conical Intersections: Electronic Structure, Dynamics & Spectroscopy*; Domcke, W., Yarkony, D. R., Köppel, H., Eds.; Advanced Series in Physical Chemistry; World Scientific: Singapore, 2004; Vol. 15, p 41.
29. Garavelli, M.; Celani, P.; Bernardi, F.; Robb, M. A.; Olivucci, M. *J. Am. Chem. Soc.* **1997**, *119*, 6891.
30. Mathics, R. A.; Lugtenburg, J. In *Handbook of Biological Physics*; Stavenga, D. G., Grip, W. J., Pugh, E. N., Eds.; Elsevier Science: Amsterdam, 2000; Vol. 3, p 55.
31. Frutos, M. L.; Andruniów, T.; Santoro, F.; Ferré, N.; Olivucci, M. *Proc. Natl. Acad. Sci. U.S.A.* **2007**, *104*, 7764.
32. Bacchus-Montabonel, M.-C.; Baech, N.; Lasorne, B.; Desouter-Lecomte, M. *Chem. Phys. Lett.* **2003**, *374*, 307.
33. Lasorne, B.; Bacchus-Montabonel, M.-C.; Vaech, N.; Desouter-Lecomte, M. *J. Chem. Phys.* **2004**, *120*, 1271.
34. Blancafort, L.; Hunt, P.; Robb, M. A. *J. Am. Chem. Soc.* **2005**, *127*, 3391.
35. Soto, J.; Arenas, J. F.; Otero, J. C.; Peláez, D. *J. Phys. Chem. A* **2006**, *110*, 8221.
36. Frisch, M. J.; Trucks, G. W.; Schlegel, H. B.; Scuseria, G. E.; Robb, M. A.; Cheeseman, J. R.; Montgomery, J. A., Jr.; Vreven, T.; Kudin, K. N.; Burant, J. C.; Millam, J. M.; Iyengar, S. S.; Tomasi, J.; Barone, V.; Mennucci, B.; Cossi, M.; Scalmani, G.; Rega, N.; Petersson, G. A.; Nakatsuji, H.; Hada, M.; Ehara, M.; Toyota, K.; Fukuda, R.; Hasegawa, J.; Ishida, M.; Nakajima, T.; Honda, Y.; Kitao, O.; Nakai, H.; Klene, M.; Li, X.; Knox, J. E.; Hratchian, H. P.; Cross, J. B.; Bakken, V.; Adamo, C.; Jaramillo, J.; Gomperts, R.; Stratmann, R. E.; Yazyev, O.; Austin, A. J.; Cammi, R.; Pomelli, C.; Ochterski, J. W.; Ayala, P. Y.; Morokuma, K.; Voth, G. A.; Salvador, P.; Dannenberg, J. J.; Zakrzewski, V. G.; Dapprich, S.; Daniels, A. D.; Strain, M. C.; Farkas, O.; Malick, D. K.; Rabuck, A. D.; Raghavachari, K.; Foresman, J. B.; Ortiz, J. V.; Cui, Q.; Baboul, A. G.; Clifford, S.; Cioslowski, J.; Stefanov, B. B.; Liu, G.; Liashenko, A.; Piskorz, P.; Komaromi, I.; Martin, R. L.; Fox, D. J.; Keith, T.; Al-Laham, M. A.; Peng, C. Y.; Nanayakkara, A.; Challacombe, M.; Gill, P. M. W.; Johnson, B.; Chen, W.; Wong, M. W.; Gonzalez, C.; Pople, J. A. *Gaussian 03 (Revision C.02.)*; Gaussian: Wallingford, CT, 2004.
37. Nakamura, K.; Osamura, Y.; Iwata, S. *Chem. Phys.* **1989**, *136*, 67.
38. Levchenko, S. V.; Krylov, A. I. *J. Chem. Phys.* **2004**, *120*, 175.
39. Nakano, H. *J. Chem. Phys.* **1993**, *99*, 7983.
40. Schmidt, M. W.; Baldridge, K. K.; Boatz, J. A.; Elbert, S. T.; Gordon, M. S.; Jensen, J. H.; Koseki, S.; Matsunaga, N.; Nguyen, K. A.; Su, S. J.; Windus, T. L.; Dupuis, M.; Montgomery, J. A. *J. Comput. Chem.* **1993**, *14*, 1347.
41. Atchity, G. J.; Xantheas, S. S.; Ruedenberge, K. *J. Chem. Phys.* **1991**, *95*, 1862.
42. Schulman, J. M.; Vnanzi, T. J. *J. Am. Chem. Soc.* **1974**, *96*, 4739.
43. Balci, M.; Mckee, M. L.; Schleyer, P. v. R *J. Phys. Chem. A* **2000**, *104*, 1246.
44. Hess, B. A., Jr.; Schaad, L. J. *J. Am. Chem. Soc.* **1985**, *107*, 865.